Bonding of α−Dicarbonyls to Nickel: Structural and Vibrational Analysis

ARTICLE *in* THE JOURNAL OF PHYSICAL CHEMISTRY A · JANUARY 2001

Impact Factor: 2.69 · DOI: 10.1021/jp002867p

2 AUTHORS:

Alain Rochefort
Polytechnique Montréal
88 PUBLICATIONS **1,935** CITATIONS
SEE PROFILE

Peter H Mcbreen
Laval University
73 PUBLICATIONS **1,231** CITATIONS
SEE PROFILE

Bonding of α-Dicarbonyls to Nickel: Structural and Vibrational Analysis

Alain Rochefort*,† and Peter McBreen‡

Centre de Recherche en Calcul Appliqué (CERCA), Groupe Nanostructures, 5160 boul. Décarie, bureau 400, Montréal (Québec), Canada H3X 2H9, and Département de Chimie, Université Laval, Cité Universitaire, Ste-Foy (Québec), Canada G1K 7P4

Received: August 8, 2000; In Final Form: December 7, 2000

The interaction between the α-dicarbonyls 2,3-butanedione, methyl pyruvate, and pyruvic acid and a single nickel atom was studied using the quantum density functional theory−generalized gradient approximation (DFT−GGA) method. With the exception of 2,3-butanedione, the most stable structure is where Ni forms a single bond with the keto carbonyl moiety. The 2,3-butanedione−Ni chelation complex is only 0.3 kcal mol^{-1} more stable than the keto-bonded configuration. The dissociation energy of the Ni−keto carbonyl complexes decreases in the order $-COCH_3 > -COOH > -COOCH_3$, in keeping with the greater electron-withdrawing ability of the $COCH_3$ substituent. The bonding properties of the different complexes are discussed in terms of charge transfer, electron delocalization, dipole interactions, and stabilizing O···H interactions. The calculated data are briefly compared to experimental data for 2,3-butanedione and methyl pyruvate on Ni(111).

I. Introduction

The asymmetric hydrogenation of α-keto esters may be accomplished by the use of homogeneous ruthenium and rhodium bearing specific chiral ligands.[1] The mechanism for the asymmetric hydrogenation of the keto group is poorly understood, but it can be assumed to involve complexation of the α-keto esters to the single metal atom complex.[1] The charge redistributions resulting from the molecule−metal interaction are of evident importance in relation to the activation of the molecule. Similarly, the structure of the metal−molecule complex is central to the stereospecifity of the reaction. Carpentier and Mortreux[1] discuss two mechanisms for the asymmetric induction; one involves chelation of the α-keto ester to the metal center, whereas the other involves attachment to the metal via only one of the two carbonyl bonds. Here, we report on the bonding of three different α-dicarbonyls ($CH_3COCOCH_3$, $CH_3COCOOCH_3$, $CH_3COCOOH$) to a nickel atom studied within the density functional theory−generalized gradient approximation (DFT−GGA) formalism. The three molecules are chosen because they are relatively simple dicarbonyls. Nevertheless, their interaction with a metal center opens up several possibilities. For example, the trans conformation is the lowest energy structure for each of the three molecules. Then, the formation of a chelation complex can only result from trans to cis isomerization. In the absence of chelation, the α-keto esters should bond to the metal center via either the keto carbonyl or the ester carbonyl group.

The purpose of the calculations described in this paper is to investigate the likehood of the various possible interactions. Several bonding schemes will be discussed in terms of energetics and structural and vibrational properties. The study was also carried out partly in relation to a surface science study of 2,3-butanedione and methyl pyruvate on Ni(111).[2,3] Vibrational data, and data for adsorption-induced rotamerization, are now available for 2,3-butanedione and methyl pyruvate on Ni(111). Hence, the present study also permits comment on whether single atom calculations are of any relevance to an understanding of the chemisorption of complex molecules on extended metal surfaces. The chemisorption of methyl pyruvate ($CH_3COCOOCH_3$) is of particular interest since its hydrogenation to methyl lactate ($CH_3CH(OH)COOCH_3$) on alkaloid-modified Pt catalysts displays very high enantioselectivities.[4−7] Similarly, hydrogenation of 2,3-butanedione to (*R*)-3-hydroxybutane-2-one occurs with 85−90% enantioselective excess on cinchona-modified Pt/Al_2O_3.[8]

II. Computational Details

The calculations were performed with the deMon-KS[9,10] software based on the linear combination of Gaussian type orbital−model core potential−generalized gradient approximation (LCGTO−MCP−GGA) formalism. The GGA functionals of Becke[11] for the exchange and the recent Lap1 scheme[12] for the correlation were employed. We used double-ζ plus polarization (DZVP) all-electron basis sets for carbon and oxygen atoms and a double-ζ (DZP) basis set for hydrogen atoms. For the nickel atom, a model core potential (MCP) that includes corrections for scalar relativistic effects[13] in conjunction with a double-ζ basis set for the valence shell was used. The contraction pattern for C and O atoms was (621/41/1*) and (41) for the H atoms. Auxiliary charge density (CD) and exchange-correlation (XC) basis sets are denoted (4,3;4,3) for carbon and oxygen and (4;4) for hydrogen. An explicit treatment of 3p, 4s, 4p, and 3d orbitals was carried out in the MCP of the Ni (Ni^{+16}) atom. The contraction pattern for the Ni atom was (311/31/311) for the valence electron orbital basis set and (3,4;3,4) for the CD and XC basis sets.

The geometries of the complexes were fully optimized by applying the energy gradient expression developed by Fournier.[14] The harmonic frequencies were determined by diagonalizing the Hessian matrix constructed by numerical differentiation of analytical gradients calculated at the equilibrium geometry. The displacement of the Cartesian coordinates in the differentiation procedure was 0.05 au. The bond dissociation energies (D_e)

† CERCA.
‡ Université Laval.

10.1021/jp002867p CCC: $20.00
Published on Web 01/27/2001

TABLE 1: Structural Properties and Stabilities of Optimized Isolated Dicarbonyl (CH_3COCOR) Conformers[j]

molecule	$(CH_3)C{=}O$ (Å)	$(R)C{=}O$ (Å)	$(O)C-C(O)$ (Å)	μ (D)	ΔE (kcal mol^{-1})	ref
trans-2,3-butanedione	1.214	1.214	1.519	0.0	0.0	this work
"*trans*-BD"	(1.214)	(1.214)	(1.507)		(0.0)	15, 16[a]
	(1.209)	(1.209)	(1.540)			17[b]
cis-2,3-butanedione	1.207	1.207	1.537	5.4	6.1	this work
"*cis*-BD"	(1.206)	(1.206)	(1.550)		(4.42)[c]	18[d]
trans-pyruvic acid	1.208	1.210	1.518	1.4	0.0	this work
"*trans*-PA"	(1.231)	(1.215)	(1.523)		(0.0)	19[e]
	(1.254)	(1.248)	(1.529)			20[f]
cis-pyruvic acid	1.206	1.201	1.524	4.2	1.7	this work
"*cis*-PA"	(1.255)	(1.241)	(1.532)		(1.28)[g]	20[f]
trans-methyl pyruvate	1.208	1.211	1.517	1.6	0.0	this work
"*trans*-MP"				(1.3)	(0.0)[h]	21
cis-methyl pyruvate	1.207	1.203	1.521	4.7	1.6	this work
"*cis*-MP"				(3.4)	(0.65)[i]	21

[a] From electron diffraction data; only the trans conformer was observed. [b] From X-ray data. [c] Ab initio STO-4G. [d] MINDO/3 calculation. [e] Obtained from microwave data; only the trans conformer was observed. [f] MP2/4-31G results. [g] MP2/6-31G** results from ref 20. [h] A fraction of cis conformer was observed in glassy, liquid, and gas phases. [i] Estimated on the basis of infrared data on liquid state. [j] The trans−cis rotational barriers calculated from a rigid rotation of the central C−C bond are 9.5, 3.1, and 3.3 for respectively 2,3-butanedione, pyruvic acid, and methyl pyruvate.

of the complexes were calculated with respect to the ground-state species asymptote. Since we focus on the relative stability of the complexes, we have not calculated the basis set superposition error (BSSE) or the zero point energy (ZPE) for correcting the dissociation energies. The energy barriers for rotation were estimated by computing the energy involved in a rigid rotation around the central C−C bond without any further optimization. The calculated values can then be considered as the upper limit for the real barriers.

III. Results and Discussion

A. Isolated Ligands. Table 1 gives the relative stabilities and the geometries of the cis−trans conformers of 2,3-butanedione (BD) ($CH_3COCOCH_3$), pyruvic acid (PA) ($CH_3COCOOH$), and methyl pyruvate (MP) ($CH_3COCO(OCH_3)$). The trans conformers are the more stable structures by only a few kcal mol^{-1} in the case of PA and MP. The higher energy difference calculated for BD (6.1 kcal mol^{-1}) suggests that the cis conformer would be practically absent (<0.01%) at 298 K, as experimentally observed.[15] The calculated trans−cis energy barrier for BD is ∼9.5 kcal mol^{-1}, which is intermediate between the experimental values of 7.6[22] and 11.4 kcal mol^{-1} [15] reported in the literature. The energy barriers computed for PA and MP (3.1 and 3.3 kcal mol^{-1}, respectively) are approximately three times lower than for BD. This result is supported by a previous studies in which a barrier of 4 kcal mol^{-1} was determined for PA from MP2/4-31G calculations[20] and about 5 kcal mol^{-1} for MP from infrared liquid-phase data.[21]

On the basis of the literature on formates and acetates, the energy differences among the BD, MP, and PA conformers may be considered in terms of dipole alignment of the carbonyl bonds[23,24] and possible contributions from steric, conjugation, and aromaticity effects.[25,26] The calculated molecular dipole moments listed in Table 1 are clearly in line with the role of carbonyl dipole alignment in determining the relative stabilities of the cis and trans conformers. Nevertheless, the GGA used here (Lap1) allows a significantly improved description of hydrogen bonds and weak interactions[12] over the local density approximation (LDA)[27] (for example, the *cis*-BD conformer becomes more stable than the *trans*-BD by 2.7 kcal mol^{-1} when the LDA is used). This result suggests that an additional contribution to the stability of the conformers could be considered such as the intramolecular O···H stabilizing interactions as illustrated in Figure 1. Dorigo et al.[28] reported calculations showing that interactions between hydrogen atoms

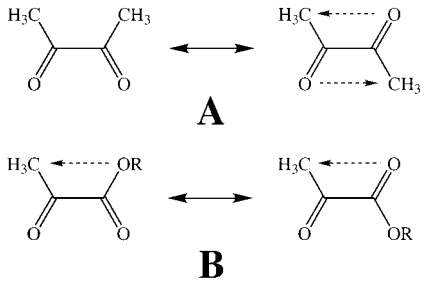

Figure 1. Effect of the R group in CH_3COCOR on the formation of intramolecular O···H interactions for 2,3-butanedione (A) and pyruvic acid and methyl pyruvate (B).

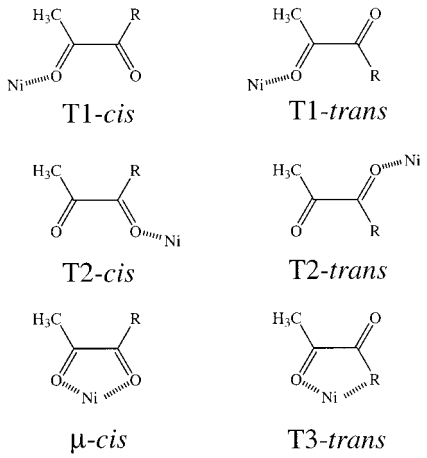

Figure 2. Structures of the Ni−dicarbonyl complexes.

on half of 2,3-butanedione with the carbonyl on the other half play a role in the CH_3C rotational barrier.

B. Ni−Dicarbonyl Complexes. The different bonding configurations of the α-dicarbonyl nickel atom complexes investigated are shown in Figure 2, while energetics and structural properties of the optimized complexes are reported in Tables 2 and 3, respectively. In general, the results predict that dicarbonyls form relatively weak bonds with nickel and that the stabilities of the different structures are within a narrow energy distribution. The bonding of dicarbonyls through a single carbonyl group in a T1 geometry is the most stable structure except for BD where the μ-cis configuration is more stable but only by 0.3 kcal mol^{-1}. The T1 geometry for MP and PA involves bonding to the keto carbonyl group. The single Ni−

TABLE 2: Relative Stability (ΔE) and Dissociation Energies (D_e) of Ni−Dicarbonyl Complexes

species	ΔE (kcal mol^{-1})	D_e (kcal mol^{-1})
2,3-butanedione (BD) (cis−trans)	6.1	
T1-*trans*-BD	0.3	38.4
T3-*trans*-BD	6.3	32.4
T1-*cis*-BD	6.4	38.3
μ-*cis*-BD	0.0	44.7
pyruvic acid (PA) (cis−trans)	1.7	
T1-*trans*-BD	0.0	37.6
T2-*trans*-PA	5.4	32.2
T1-*cis*-PA	1.7	37.6
T2-*cis*-PA	6.7	32.6
μ-*cis*-PA	7.9	31.4
methyl pyruvate (MP) (cis−trans)	1.6	
T1-*trans*-MP	0.0	36.5
T2-*trans*-MP	9.4	27.1
T3-*trans*-MP	2.5	34.0
T1-*cis*-MP	1.4	36.7
T2-*cis*-MP	11.3	26.8
μ-*cis*-MP	8.5	29.6

OC-bonded complexes show an Ni−O−C angle (130−135°) that intuitively suggests bonding of Ni to an electron lone pair of oxygen,[29,30] since this range of M−O−C angles is in line with experimental observations for carbonyl−Lewis acid complexes.[31] However, the distribution of charges and the bond order (BO) listed in Tables 4 and 5 show a net charge transfer from nickel to oxygen. The overall result is a significant decrease in the BO of the CO bond and an increase in the BO of the central C−C bond. This implies that there is back-donation from the Ni to the carbonyl π^* orbital in addition to transfer of electron density from the oxygen lone pair to the metal. In terms of equilibrium geometries, bonding to nickel systematically induces an elongation of the C═O bonds and a contraction of the central C−C bond. The magnitude of these changes is greater for Ni−keto carbonyl bonding.

The nature of the R group in COR has a significant influence on the strength of the Ni−O bond formed (see Table 2). The largest variations occur for T2 (Ni−OCR) complexes where the dissociation energy (D_e) decreases as CH_3 > OH > OCH_3 in the trans and cis series. This trend is also observed in the μ-complexes and to a much lower extent in the T1 complexes. The variation of D_e for the T2 complexes as a function of the nature of the R group follows the polarity of the COR carbonyl bond in the isolated ligands. As shown in Table 4, the charge separation (or internal dipole moment) in the C═O(R) carbonyl group increases as CH_3 < OH < OCH_3, suggesting that the bonding of nickel to a strongly polarized carbonyl group leads to a weak Ni−O bond. The increasing polarity of the C−O bond suggests a decrease of its capacity to accommodate additional electron charge. This result is reminiscent of previous experimental studies showing a decrease in chemisorption energy from acetone $(CH_3)_2CO$ to hexafluoroacetone $(CF_3)_2CO$ when adsorbed on an electron-withdrawing metal surface such as Pt(111)[32] and Ru(001).[33] This behavior was explained by a decreasing electron density around oxygen due to the presence of electron-withdrawing CF_3 groups which attenuate the charge transfer from oxygen lone pairs to the electroattractive metal surface. Here, we observe the complementary but converse behavior that the presence of electron-rich groups (OH, OCH_3, CH_3) induces an electron enrichment on O atom that attenuates the carbonyl group ability to accommodate incoming charge from the Ni atom.

1. Ni−2,3-Butanedione (Ni−BD). As mentioned above, the μ-cis complex is more stable than the T1-trans configuration only by 0.3 kcal mol^{-1}. This result is in good agreement with observation by Carpentier and Mortreux[1] that α-keto esters do not form chelation complexes with Rh−AMPP catalysts. In contrast, a W−2,3-butandione chelation complex has been isolated.[34] This small energy difference is much lower than the relative energy difference between the isolated cis−trans conformers (6.1 kcal mol^{-1}) and the calculated trans to cis rotational barrier conformation (≤9.5 kcal mol^{-1}). In addition, the T3-trans and T1-cis structures which may be viewed as intermediate geometries in a T1-trans to μ-cis transition are less stable by ≈6 kcal mol^{-1}. Given that isolated *trans*-BD is the more stable conformer, the T1-trans structure is predicted to form more easily than μ-cis due to the absence of an energy barrier. The higher stability of the μ-cis complex with respect to other complexes is related to the greater Ni−O coupling that favors the π_{CO}^* back-donation,[33] the delocalization of π-electrons among the O═C−C═O fragment,[34] and the reduction of the repulsion between carbonyl dipoles.[23] From Tables 4 and 5, one can see the substantial charge transfer from strongly rehybridized nickel to oxygen atoms that contributes to the decrease in the bonding order (BO) of both C═O bonds (BO

TABLE 3: Structural Properties of Optimized Ni−Dicarbonyl Complexes

species[a]	(CH_3)C═O (Å)	(R)C═O (Å)	(O)C−C(O) (Å)	Ni−O (Å)	∠Ni−O−C (deg)	μ (D)
trans-BD	1.214	1.214	1.519			0.0
T1-*trans*-B D	1.263	1.225	1.463	1.711	131	3.0
T3-*trans*-B D	1.260	1.227	1.467	1.711	139	2.6
cis-BD	1.207	1.207	1.537			5.4
T1-*cis*-BD	1.257	1.219	1.475	1.708	133	4.6
μ-*cis*-BD	1.296	1.297	1.401	1.828/1.831	107/107	0.5
trans-PA	1.208	1.210	1.518			1.4
T1-*trans*-PA	1.259	1.217	1.459	1.713	131	1.8
T2-*trans*-PA	1.216	1.256	1.476	1.732	123	3.6
cis-PA	1.206	1.201	1.524			4.2
T1-*cis*-PA	1.256	1.210	1.466	1.706	133	3.3
T2-*cis*-PA	1.215	1.248	1.479	1.732	123	3.7
μ-*cis*-PA	1.291	1.272	1.409	1.827/1.896	109/105	1.1
trans-MP	1.208	1.211	1.517			1.6
T1-*trans*-M P	1.257	1.218	1.463	1.709	132	1.3
T2-*trans*-M P	1.217	1.250	1.474	1.723	137	3.6
T3-*trans*-M P	1.259	1.218	1.459	1.712/2.783	135	2.0
cis-MP	1.207	1.203	1.521			4.7
T1-*cis*-MP	1.255	1.210	1.466	1.706	133	3.3
T2-*cis*-MP	1.216	1.241	1.476	1.722	137	5.1
μ-*cis*-MP	1.290	1.270	1.413	1.830/1.897	109/105	1.6

[a] BD = 2,3-butanedione, PA = pyruvic acid, and MP = methyl pyruvate.

TABLE 4: Distribution of Net Charges in Nickel−Dicarbonyl Complexes

species[a]	$(CH_3)C^b$	$(CH_3C)O^b$	$C^b(R)$	$O^b(CR)$	Ni (4s, 4p, 3d)
trans-BD	−0.01	−0.24	−0.01	−0.24	
T1-*trans*-BD	+0.02	−0.38	−0.02	−0.27	+0.15 (0.67, 0.08, 9.10)
T3-*trans*-BD	+0.02	−0.38	−0.03	−0.27	+0.14 (0.64, 0.11, 9.11)
cis-BD	−0.02	−0.20	−0.02	−0.20	
T1-*cis*-BD	+0.00	−0.32	−0.04	−0.24	+0.16 (0.66, 0.09, 9.09)
μ-*cis*-BD	−0.01	−0.43	−0.01	−0.43	+0.41 (0.47, 0.25, 8.88)
trans-PA	+0.03	−0.20	+0.17	−0.28	
T1-*trans*-PA	+0.07	−0.34	+0.17	−0.31	+0.16 (0.66, 0.08, 9.10)
T2-*trans*-PA	+0.00	−0.23	+0.27	−0.38	+0.07 (0.69, 0.09, 9.15)
cis-PA	+0.03	−0.20	+0.17	−0.25	
T1-*cis*-PA	+0.05	−0.32	+0.17	−0.29	+0.16 (0.65, 0.08, 9.10)
T2-*cis*-PA	+0.00	−0.23	+0.27	−0.33	+0.08 (0.68, 0.09, 9.15)
μ-*cis*-PA	+0.06	−0.41	+0.22	−0.44	+0.36 (0.45, 0.23, 8.96)
trans-MP	+0.02	−0.21	+0.18	−0.30	
T1-*trans*-MP	+0.05	−0.34	+0.19	−0.32	+0.15 (0.67, 0.08, 9.10)
T2-*trans*-MP	−0.01	−0.24	+0.23	−0.39	+0.06 (0.65, 0.11, 9.18)
T3-*trans*-MP	+0.03	−0.35	+0.19	−0.32	+0.19 (0.63, 0.09, 9.09)
cis-MP	0.00	−0.20	+0.20	−0.27	
T1-*cis*-MP	+0.02	−0.32	+0.20	−0.30	+0.15 (0.66, 0.08, 9.11)
T2-*cis*-MP	−0.02	−0.25	+0.23	−0.34	+0.07 (0.63, 0.12, 9.18)
μ-*cis*-MP	+0.03	−0.41	+0.24	−0.45	+0.35 (0.45, 0.24, 8.96)

[a] BD = 2,3-butanedione, PA = pyruvic acid, and MP = methyl pyruvate. [b] Net charge on this atom.

TABLE 5: Mayer's Bond Orders in Nickel−Dicarbonyl Complexes

species[a]	$(CH_3)C-O$	$(CH_3)C-C(R)$	$(R)C-O$	Ni−O
trans-BD	2.09	0.94	2.09	
T1-*trans*-BD	1.48	1.09	1.99	0.72
T3-*trans*-BD	1.53	1.06	2.00	0.68
cis-BD	2.16	0.90	2.16	
T1-*cis*-BD	1.55	1.04	2.09	0.73
μ-*cis*-BD	1.23	1.39	1.23	0.61/0.61
trans-PA	2.15	0.89	2.03	
T1-*trans*-PA	1.55	1.03	1.97	0.72
T2-*trans*-PA	2.09	0.99	1.50	0.64
cis-PA	2.18	0.88	2.10	
T1-*cis*-PA	1.57	1.01	2.04	0.72
T2-*cis*-PA	2.10	0.98	1.55	0.66
μ-*cis*-PA	1.32	1.22	1.47	0.59/0.46
trans-MP	2.15	0.91	1.97	
T1-*trans*-MP	1.56	1.04	1.92	0.71
T2-*trans*-MP	2.08	1.01	1.51	0.60
T3-*trans*-MP	1.54	1.04	1.94	0.71/0.06
cis-MP	2.16	0.91	2.03	
T1-*cis*-MP	1.57	1.03	1.98	0.72
T2-*cis*-MP	2.09	1.00	1.57	0.62
μ-*cis*-MP	1.32	1.23	1.44	0.58/0.45

[a] BD = 2,3-butanedione, PA = pyruvic acid, and MP = methyl pyruvate.

= 1.23) and to an increase for the central C−C bond (BO = 1.39) as in a delocalized π-system. This charge redistribution significantly improves the stability of the complex as seen from the dissociation energy (D_e) in Table 2.

2. Ni−Pyruvic Acid (Ni−PA) and Ni−Methyl Pyruvate (Ni−MP). The energy difference between trans and cis conformers of isolated PA is relatively small (1.7 kcal mol^{-1}) as is the rotation barrier ($\leq$3.1 kcal mol^{-1}). The most stable complexes display T1 structures which are separated by 1.7 kcal mol^{-1} corresponding exactly to the energy difference as between the isolated trans and cis species. The two T1 complexes display the same dissociation energy (37.6 kcal mol^{-1}). Since the charge transfer from Ni to O is smaller in T2 (see Table 4), this leads to a weaker Ni−O bond, and consequently, the variations in bonding properties (bond length, charges distribution, and BOs) of other bonds are smaller than for the T1-structures. Finally, *μ*-*cis*-PA represents the least stable structure, as well as the one easiest to dissociate (D_e = 31.4 kcal mol^{-1}) of the Ni−PA complexes investigated. Table 4 reveals similar charge transfer from Ni to both O atoms, but Ni tends to form a stronger bond (see Table 5) with the $(CH_3)CO$ keto fragment (BO = 0.59) than with the CO(OH) acid group (BO = 0.46). Similarly, the Ni−O bond length is shorter (R_e = 1.827 Å) for Ni−OC(CH_3) than for Ni−OC(OH) (R_e = 1.896 Å). The results obtained with Ni−MP complexes are quite similar to those obtained on the Ni−PA complexes. The T1-structures are the most stable, and the trans and cis conformers are separated by a slightly lower energy (1.4 kcal mol^{-1}) than for the isolated MP species (1.6 kcal mol^{-1}). The bonding of Ni in a T2-structure is much less favored, and we can easily relate their low stability and their large Ni−O−C angles (137°), with respect to T2-PA complexes (123°), to the low ability of the $-COOCH_3$ moiety to accept incoming charge. On the other hand, the two T2-conformers show very similar bonding properties. The Ni−O bond is longer in Ni−OC(OCH_3) than in Ni−OC(CH_3) and reflects a weaker Ni−O interaction as the CO bond becomes more polarized and less available to accommodate an incoming charge.

C. Vibrational Properties. We limit our description of the vibrational spectra to the group frequencies that are directly related to the bonding of the different ligands to the nickel atom. The computed infrared vibrational frequencies for carbonyl groups and for the central C−C bond are presented in Table 6. Both isolated *cis*- and *trans*-BD give similar C═O stretching frequencies of about 1825 cm^{-1} which is 5% higher than the experimental gas-phase data (1734 cm^{-1}).[35] However, there are large differences between our calculated value and experimental data for the central C−C stretching frequency. The assignment of the ν(CC) band from experimental data does not appear to be trivial since bands at 1000 cm^{-1} for BD and MP[21,35,36] and at 1355 cm^{-1}[37] for PA have been attributed to C−C stretching. Bonding to Ni in a T1 structure induces a decrease in the C═O frequency of around 200 cm^{-1} and of approximately 40−80 cm^{-1} in the second C═O group. The variation in the vibrational frequencies for CO or CC is also in agreement with the various changes of bonding properties discussed above. They are clearly related to the charge transfer from nickel to oxygen via the π^* antibonding orbitals of the CO moiety leading to a decrease in the C═O bond order, an elongation of the C═O bond length, and consequently a decrease in its vibrational frequency.

TABLE 6: Vibrational Frequencies of Ni−Dicarbonyl Complexes

species[a]	$(CH_3)C{=}O$ (cm^{-1})	$(O)C{-}C(O)$ (cm^{-1})	$(R)C{=}O$ (cm^{-1})
trans-BD	1824 (1734)[b]	1264 (1005)[c]	1824 (1734)[b]
T1-*trans*-BD	1604	1277	1752
T3-*trans*-BD	1620	1279	1742
cis-BD	1826	1239	1826
T1-*cis*-BD	1617	1279	1783
μ-*cis*-BD	1458	1297	1458
trans-PA	1851 (1800)[d]	1210 (1355)[d]	1844 (1729)[d]
T1-*trans*-PA	1630	1232	1803
T2-*trans*-PA	1796	1226	1652
cis-PA	1889	1179	1858
T1-*cis*-PA	1640	1207	1836
T2-*cis*-PA	1804	1196	1668
μ-*cis*-PA	1525	1232	1563
trans-MP	1855 (1741)[e]	1207 (1000)[e]	1835 (1737)[e]
T1-*trans*-MP	1641	1229	1796
T2-*trans*-MP	1789	1223	1659
T3-*trans*-MP	1624	1222	1783
cis-MP	1873 (1762)[e]	1197 (964)[e]	1853 (1733)[e]
T1-*cis*-MP	1640	1218	1826
T2-*cis*-MP	1795	1209	1686
μ-*cis*-MP	1504	1237	1555

[a] BD = 2,3-butanedione, PA = pyruvic acid, and MP = methyl pyruvate. [b] Gas-phase IR.[35] [c] Liquid-phase IR.[35] [d] Argon matrix data.[37] [e] Liquid-phase IR.[21]

It is interesting to note that both donor and acceptor interactions would lead to a similar trend for C═O and C−C vibrational bands. A charge transfer from the ligand to the metal would remove a partial charge from the HOMO (a lone pair or n_O orbital) resulting in a decrease in the strength of the C═O bond.[38,39] On the other hand, a charge transfer from Ni to the ligand necessitates the participation of the low-lying LUMO orbital of carbonyls (π_{CO}*) to accommodate the incoming charge. Such an increasing antibonding character makes the C═O bond weaker. This mechanism is emphasized in the case of the bidentate μ-complex in which a large charge transfer occurs causing both C═O vibrational frequencies to decrease sharply by around 370 cm^{-1}. The higher increase for the central C−C of μ-BD ($\approx$60 cm^{-1}) agrees also with an improved delocalized π-system within the O═C−C═O chelation complex formed with the Ni atom. The calculated ν(C−C) frequency is much lower than the frequency (1600 cm^{-1}) assigned to the CC vibration of 2,3-butanedione chelated to a W complex.[34] The observed C═O and central C−C bond lengths for the W−chelation complex are approximately 1.37 and 1.33 Å, consistent with a stronger molecule−W interaction than that predicted for Ni. Table 3 shows that the respective bond lengths for the Ni−chelation complex are 1.3 and 1.4 Å. This difference is probably partly due to the greater spatial extension of the third-row element orbitals. Figure 3 gives a general representation of the molecular orbitals formed, for the μ-complexes, from the interaction of nickel atom with CH_3COCOR ligands. In this interaction, Ni becomes strongly rehydridized in order to facilitate charge transfer into the empty π* orbital of CO through a back-donation mechanism. Obviously, the magnitude of the π_{CO}* back-donation is related to the degree of Ni−O coupling which, for example, is greater in the μ-complexes than in the T1-complexes. This contrasts somewhat with the idea that π_{CO}* back-donation occurs mainly for η_2-complexes (where the C═O bond is parallel to the surface).[33]

The changes in vibrational frequencies for PA and MP complexes follow a similar trend to those outlined for the BD complexes. However, the decrease in the C═O frequencies is larger for $RCO(CH_3CO)$−Ni complexes than for (CH_3CO)-RCO−Ni complexes. For example, in the *cis*-MP complexes, bonding in a T1 geometry decreases the keto C═O frequency by 233 cm^{-1} while it decreases by 167 cm^{-1} in the T2 geometry. Similarly, the CO frequency of $(CH_3)C{=}O$ decreases by 369 cm^{-1} with respect to 298 cm^{-1} for COR in the μ-complex. This difference can be easily explained by a larger charge transfer from Ni to CO in $CH_3C{=}O$ than in COR. The larger charge transfer can be understood by a greater participation of the π_{CO}* orbital in the bonding. In contrast, the CO frequency in $CH_3C{=}O$ of the T2 conformation decreases by 78 cm^{-1} with respect to the moderate decrease of 27 cm^{-1} of COR in T1. This behavior is related to the driving force that redistributes electron density from the Ni atom into the more electroattractive region of PA and MP molecules which corresponds to the RCO moiety.

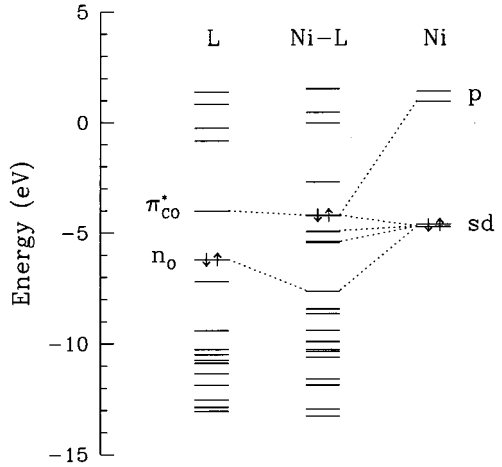

Figure 3. General molecular orbital diagram of Ni−dicarbonyl complexes. (Only valence electrons are represented.)

IV. Conclusions

We have studied the bonding between α-dicarbonyls and a single nickel atom using the LCGTO−MCP−GGA method. The most stable configuration involves a single bond to the keto CO through the oxygen lone pair and π_{CO}*-back-donation rather than bidentate complexation, except in the case of 2,3-butanedione. However, even in the latter case, the T1-structure is only 0.3 kcal mol^{-1} less stable than the chelate structure. This result is consistent with experimental observation for the α-keto ester Rh single metal complexes. A contribution to the energy difference between isolated or bonded cis−trans conformers arises from their ability to form intramolecular O···H interactions. The main characteristic of the metal−ligand bonding is the charge transfer from Ni to the dicarbonyls and the redistribution of this incoming charge into the entire molecule. Furthermore, complexation occurs preferentially through the keto carbonyl in the case of MP and PA. However, as shown in Table 4, bonding through the ester carbonyl leads to some change in charge density at the keto carbonyl oxygen. The nature of the electron-accepting group (−COR) adjacent to the keto carbonyl group was found to significantly affect the binding energy of Ni complexes. The binding energy of the Ni−keto carbonyl bonds follows the order $-COCH_3 > -COOH > -COOCH_3$, which is directly related to the increasing ability of those fragments to withdraw electrons. The charge tranfer induces several structural changes in the ligands such as an elongation of CO bond and a contraction of the central C−C bond length. These changes are more marked in μ-cis complexes in which substantial π-electron delocalization is observed in O═C−C═O fragment. The vibrational properties of the complexes

are directly related to the structural changes observed: the CO frequency is strongly red-shifted for the carbonyl where Ni is attached while the C−C stretching frequency is slightly blue-shifted. The predicted changes in the ν(CO) stretching frequencies are about twice those observed for 2,3-butanedione and methyl pyruvate on Ni(111). Furthermore, both of these molecules are observed to form cis-adsorbed states on Ni(111). The discrepancy between the calculated frequencies and the surface science data could have a number of origins. First, a single metal atom cannot be expected to take into account the full complexity of charge redistribution between a chemisorbed molecule and a bulk metal. Second, for relatively large molecules such as those under study, steric effects will lead to different metal−molecule bond angles for the single metal atom model as compared to an extended surface. Third, the noncovalent interaction of the large molecule and the extended surface will evidently be greater than that between the same molecule and a single metal atom. Thus, even for a diketone bonded to the surface via one carbonyl, the overall adsorption geometry will reflect the optimal sum of the carbonyl group−metal chemisorption and the molecule−metal noncovalent forces. A single metal atom model, as used in the present study, may overemphasize geometries permitting a extensive metal−carbonyl back-bonding interaction, thereby predicting low carbonyl vibrational frequencies. The calculated charge redistributions (Table 4) do, in fact, show a large back-donation component. In contrast, chemisorption on an extended surface may result in a geometry which leads to a smaller back-donation component and, hence, higher carbonyl vibrational frequencies. Thus, it is clear that calculations involving cluster models, rather than single atoms, are required to correctly model the case of an extended surface. The present results are however sufficient to contribute to an eventual understanding of asymmetric hydrogenation of α-keto esters and related molecules at single metal centers.

References and Notes

(1) Carpentier, J.-F.; Mortreux, A. *Tetrahedron:Asymmetry* **1997**, *8*, 1083.

(2) Castonguay, M.; Roy, J. R.; Rochefort, A.; McBreen, P. H. *J. Am. Chem. Soc.* **2000**, 122, 518.

(3) Roy, J.-R.; Castonguay, M.; Rochefort, A.; McBreen, P. H. Manuscript in preparation.

(4) Orito, Y.; Imai, S.; Niwa, S. *J. Chem. Soc. Jpn.* **1979**, 1118.

(5) Baiker, A.; Blaser, H. U. Enantioselective Catalysis and Reactions. In *Handbook of Heterogeneous Catalysis and Reaction*; Ertl, G., Knözinger, H., Weitkamp, J., Eds.; VCH Publishers: Weinheim, Germany, 1997; Vol. 5, p 2422.

(6) LeBlond, C.; Wang, J.; Andrews, A. T.; Sun, Y.-K. *J. Am. Chem. Soc.* **1999**, *121*, 4920.

(7) Zuo, X.; Liu, H.; Liu, M. *Tetrahedron Lett.* **1998**, *39*, 1941.

(8) Studer, M.; Okafor, V.; Blaser, H. U. *Chem. Commun.* **1998**, 1053.

(9) St-Amant, A.; Salahub, D. R. *Chem. Phys. Lett.* **1990**, *169*, 387.

(10) St-Amant, A. Ph.D. Thesis, Université de Montréal, 1991.

(11) Becke, A. D. *Phys. Rev. A* **1988**, *38*, 3098.

(12) Proynov, E. I.; Ruiz, E.; Vela, A.; Salahub, D. R. *Int. J. Quant. Chem. Symp.* **1995**, *29*, 61.

(13) Andzelm, J.; Radzio, E.; Salahub, D. R. *J. Chem. Phys.* **1985**, *83*, 4573.

(14) Fournier, R.; Andzelm, J.; Salahub, D. R. *J. Chem. Phys.* **1989**, *90*, 6371.

(15) Hagen, K.; Hedberg, K. *J. Am. Chem. Soc.* **1973**, *95*, 8266.

(16) Danielson, D. D.; Hedberg, K. *J. Am. Chem. Soc.* **1979**, *101*, 3730.

(17) Eriks, K.; Hayden, T. D.; Hsi Yang, S.; Chan, I. Y. *J. Am. Chem. Soc.* **1983**, *105*, 3940.

(18) Tyrrell, J. *J. Am. Chem. Soc.* **1979**, *101*, 3766.

(19) Dillick-Brenzinger, C. E.; Bauder, A.; Günthard, Hs. H. *Chem. Phys.* **1977**, *23*, 195.

(20) Murto, J.; Raaska, T.; Kunttu, H.; Räsänen, M. *J. Mol. Struct. (Theochem)* **1989**, *200*, 93.

(21) Wilmshurst, J. K.; Horwood, J. F. *Aust. J. Chem.* **1971**, *24*, 1183.

(22) Henderson, G. L.; Meyer, G. H. *J. Phys. Chem.* **1976**, *80*, 2422.

(23) Wiberg, K. B.; Laidig, K. E. *J. Am. Chem. Soc.* **1987**, *109*, 5935.

(24) Wiberg, K. B.; Wong, M. W. *J. Am. Chem. Soc.* **1993**, *115*, 1078.

(25) Pawar, D. M.; Khalil, A. A.; Hooks, D. R.; Collins, K.; Elliot, T.; Stafford, J.; Smith, L.; Noe, E. A. *J. Am. Chem. Soc.* **1998**, *120*, 2108.

(26) Epiotis, N. D.; Cherry, W. R.; Shaik, S.; Yates, R. L.; Bernardi, F. *Top. Curr. Chem.* **1977**, *70*, 1.

(27) Vosko, S. H.; Wilk, L.; Nusair, N. *Can. J. Phys.* **1980**, *58*, 1200.

(28) Dorigo, A. E.; Pratt, D. W.; Houk, K. N. *J. Am. Chem. Soc.* **1987**, *109*, 6591.

(29) Fleck, L. E.; Ying, Z. C.; Feehery, M.; Dai, H. L. *Surf. Sci.* **1993**, *296*, 400.

(30) Lepage, T. J.; Wiberg, K. B. *J. Am. Chem. Soc.* **1988**, *110*, 6642.

(31) Shambayati, S.; Crowe, S.; Schreiber, S. L. *Angew. Chem., Int. Ed. Engl.* **1990**, *29*, 256.

(32) (a) Avery, N. R. *Surf. Sci.* **1983**, *125*, 771. (b) Avery, N. R. *Langmuir* **1985**, *1*, 162.

(33) Walczak, M. M.; Leavitt, P. K.; Thiel, P. A. *J. Am. Chem. Soc.* **1987**, *109*, 5621 and references therein.

(34) Chisholm, M. H.; Huffman, J. C.; Ratermann, A. L. *Inorg. Chem.* **1983**, *22*, 4100.

(35) Durig, J. R.; Hannum, S. E.; Brown, S. C. *J. Phys. Chem.* **1971**, *75*, 1946.

(36) Allinger, N. L.; Fan, Y. *J. Comput. Chem.* **1994**, *15*, 251.

(37) Holleinstein, H.; Akermann, F.; Günthard, Hs.H. *Spectrochim. Acta, Part A* **1978**, *34*, 1041.

(38) Zahidi, E.; Castonguay, M.; McBreen, P. H. *J. Am. Chem. Soc.* **1994**, *116*, 5847.

(39) Meaume, M. T.; Odiot, S. *J. Mol. Struct.* **1972**, *11*, 147.